DOI: 10.1002/ejoc.201001525

# Study of the Structure and Photochemical Decomposition of Azidoadamantanes Entrapped in α- and β-Cyclodextrin

Udo H. Brinker,*[a] Peter Walla,[a] Daniel Krois,[a] and Vladimir B. Arion[b]

**Keywords:** Supramolecular chemistry / Azides / Imines / Cyclodextrins / Circular dichroism

Photolysis of 1-azidoadamantane (**1**), either in its neat state or in alkane solution, yields the dimeric product **4**. In contrast, amino alcohol **3** is formed as the sole product in high yield when **1** is confined within cyclodextrins (CyDs). To understand the discrepancy in product distribution caused by supramolecular encapsulation, CyD inclusion complexes (ICs) of azidoadamantanes were fully characterized. Indeed, intermolecular selectivity was influenced by reactant orientation and mobility. Both, 1- (**1**) and 2-azidoadamantane (**5**) yield 1:1 ICs with β-CyD and 1:2 ICs with α-CyD. As inferred from 2-D ROESY spectra in $D_2O$, **1** is accommodated at the wider rim of β-CyD with the azido group pointing into the cavity. However, two principal orientations of **5** inside the cavity of β-CyD were found. Single crystal X-ray analysis of solid **5** also demonstrates a bimodal orientation within β-CyD. In addition, the first induced circular dichroism (ICD) study of an alkyl azide entrapped within CyD cavities is reported. From these data, it was concluded that azide **1** is bound more strongly within β-CyD in $H_2O$/EtOH = 8:2 at 293 K ($K_a = 20240 \pm 1000\ M^{-1}$) than is 2-azidoadamantane (**5**) ($K_a = 7450 \pm 400\ M^{-1}$).

## Introduction

Azides[1] have served as nitrene[2] precursors for quite some time. The reactive intermediates are generated after elimination of molecular nitrogen by either thermal or photochemical methods. These electron-deficient species can react immediately with surrounding molecules, thus making them useful photoaffinity labels.[3,4]

Cyclodextrins (CyDs) are cyclic oligosaccharides made through the glycosidic 1→4 linkage of α-D-glucopyranose monomers. The truncated cone-shaped structures possess a hydrophobic interior comprising fugacious water molecules that readily escape when substituted by less polar guest molecules.[5] The ability to include organic molecules within CyDs has long been exploited by commercial industries, thereby ensuring a bright future for these useful inclusion compounds.[6]

It has already been shown that CyDs can dramatically alter the reaction pathways of carbene intermediates entrapped within them.[7] One therefore wonders whether the selectivity of the reactions of azidoadamantanes **1** and **5** or their corresponding nitrene intermediates will be altered as well. Herein, we demonstrate that supramolecular confinement of these species by CyDs does indeed change their reactivity. We also investigated whether photoaffinity labeling occurred, by innermolecular reaction between guest and host, leading to modified CyDs. To further our knowledge about these supramolecular aggregates, correlations of the geometry inferred from 2-D ROESY measurements with induced circular dichroism (ICD) spectra are described. Finally, the association constant ($K_a$) values for **1** and **5** with β-CyDs were determined by ICD.

[a] Lehrstuhl für Physikalisch-Organische Chemie und Strukturchemie, Institut für Organische Chemie, Universität Wien,
Währinger Straße 38, 1090 Wien, Austria
Fax: +43-1-4277-52140
E-mail: udo.brinker@univie.ac.at
[b] Institut für Anorganische Chemie, Universität Wien,
Währinger Straße 42, 1090 Wien, Austria
Supporting information for this article is available on the WWW under http://dx.doi.org/10.1002/ejoc.201001525.

## Results and Discussion

Photolysis of 1-azidoadamantane (**1**) initiates the expulsion of $N_2$ and results in the temporary formation of 4-azatricyclo[4.3.1.1$^{3,8}$]undec-3-ene (**2**) (Scheme 1). This occurs either in one step or in two steps involving the intermediate 1-adamantanylnitrene. Further reaction of unstable bridgehead imine **2** depends on its surroundings. Addition by an adventitious water molecule leads to the formation of 4-azatricyclo[4.3.1.1$^{3,8}$]undecan-3-ol (**3**).[8] Under anhydrous conditions, dimerization yields 9,18-diaza-2,6:4,9:12,16,14,18-tetramethanodispiro[7.7.1.1]octadecane (**4**), which features a 1,3-diazetidine core indicative of a head-to-tail cycloaddition.[9] Hence, the photolysis of **1** either in the solid state or in an alkane solution afforded dimer **4** only (Table 1, entries 1, 2).

In stark contrast, however, photolysis of solid **1**@β-CyD and **1**@(α-CyD)$_2$ ICs afforded **3** exclusively (Table 1, entries 3, 4). Clearly, using CyDs significantly altered the reaction pathway of the intermediate generated from **1** inside the host cavity. A confined, reactive intermediate lacks the time

  

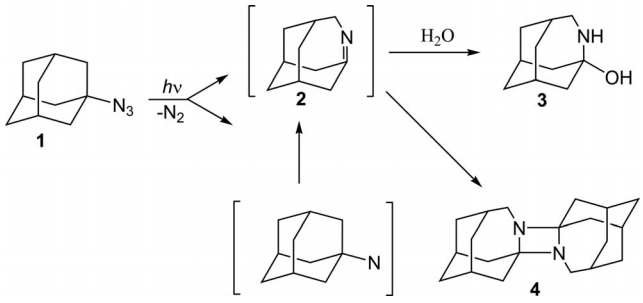


Scheme 1. Photolyses products of **1**.

Table 1. Photolyses products of azidoadamantanes **1** and **5**.

| Entry | | Yield [%][a] | | | |
|---|---|---|---|---|---|
| | | **3** | **4** | **6** | **8** |
| 1 | **1** (solid state) | – | 84 | – | – |
| 2 | **1** (alkane solution) | – | 88 | – | – |
| 3 | **1**@(α-CyD)$_2$ | 94[b] | – | – | – |
| 4 | **1**@β-CyD | 91 | traces | – | – |
| 5 | **5** (solid state) | – | – | 84 | 15 |
| **6** | **5** (alkane solution) | – | – | 87 | 5 |
| 7 | **5**@(α-CyD)$_2$ | – | – | 81 | 10 |
| **8** | **5**@β-CyD | – | – | 77 | 23 |

[a] Yields were determined by quantitative analytical GC-FID. [b] Traces of 1-adamantanamine and 1-adamantanol were detected by GC-MS.

and ability to interact with other intermediates or their precursors. So, intermediate **2** cannot dimerize to give **4** due to its incarceration. This behavior differs from aziadamantanes, which form very strong ICs with β-CyD but are nevertheless positioned within the crystal lattice to form azines.[10] For the 1:2 complexes with α-CyD any kind of dimerization becomes impossible for aziadamantanes as well as for **1** and **5**. Without recourse, imine **2** is forced to react with fortuitous water molecules co-entrapped in CyD to afford **3** as the sole product in high yield. It should be noted that in aqueous alcohol, a protic solvent, photolysis of **1** also yields **3**.[9]

Photodecomposition of 2-azidoadamantane (**5**) affords the imine **6** (4-azatricyclo[4.3.1.1$^{3,8}$]undec-4-ene, see Scheme 2), which neither reacts with water nor does it dimerize. Due to the presence of an α-H atom, however, **5** also forms the exocyclic imine 2-iminoadamantane (**7**) to a minor extent. This hydride migration occurs either in one step or in two steps involving the intermediate 2-adamantanylnitrene. Imine **7** is readily hydrolyzed during aqueous work-up to give adamantanone (**8**).[11]

In contrast to that of **1**@CyD, the photolysis of **5**@CyD essentially led to the same product distribution of **6** and **8** (Table 1, entries 7, 8) as that of the classical solution chemistry (Table 1, entry 6). Thus, neither α- nor β-CyDs alter the reaction's outcome.

ESI MS and HPLC analyses of the CyD fraction from the photodecomposition of **1**@CyD and **5**@CyD ICs clearly revealed the absence of modified CyDs. Consequently, there is no interaction between the reactant and its host molecule. This is truly unlike the decomposition

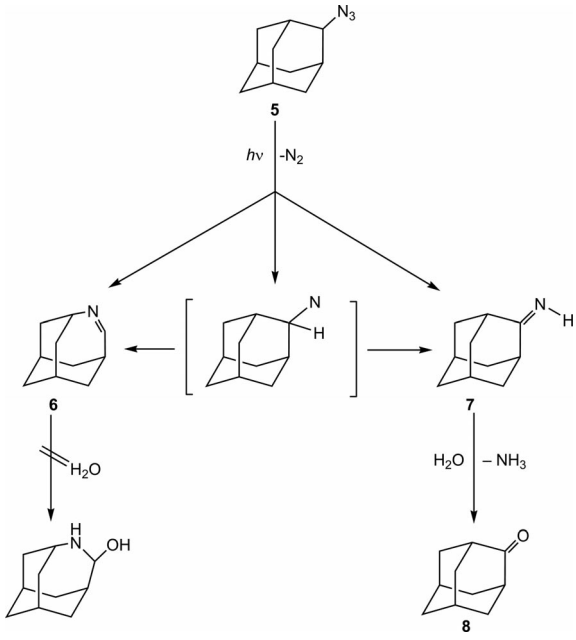


Scheme 2. Photolyses products of **5**.

conducted with the aziadamantane@α-CyD IC, for which a chemospecific insertion of adamantanylidene into the CyD's 3-OH and 2-OH bonds takes place.[10,12]

Physical methods, such as X-ray diffraction, two-dimensional rotating-frame Overhauser effect spectroscopy (2-D ROESY), and induced circular dichroism (ICD) were employed to help understand the relationship between structure and reactivity. The assemblies of the ICs of adamantane azides **1** and **5** with β-CyD could be inferred from 2-D ROESY experiments, which were conducted in $D_2O$ at 300 K (Figures 1 and 2). The spectra for **1** and **5** showed cross-peaks with the inner β-CyD protons H3 and H5, which are indicative of true inclusion. Thus, a straightfor-

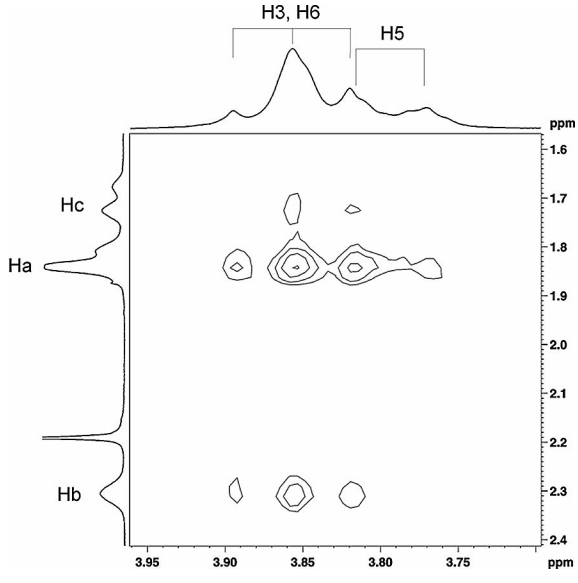


Figure 1. 250 MHz 2-D ROESY spectrum of **1**@β-CyD in $D_2O$. Mixing time 600 ms.

  

ward proposal for the geometry of **1**@β-CyD could be made (Figure 3). In contrast, interpretation of the 2-D ROESY spectrum of **5**@β-CyD did not suggest a single geometry of this IC. Two possible orientations of the guest molecule could account for the observed cross-signals in the 2-D ROESY spectrum (Figure 4). Further analysis using single-crystal X-ray diffraction techniques was warranted.

Colorless prismatic crystals of **5**@β-CyD were obtained after cooling a hot aqueous:ethanolic solution of **5** and β-CyD. They were of the composition $2\beta\text{-CyD}\cdot 0.75C_{10}H_{15}N_3\cdot 21.5H_2O$ and could be assigned to the tri-

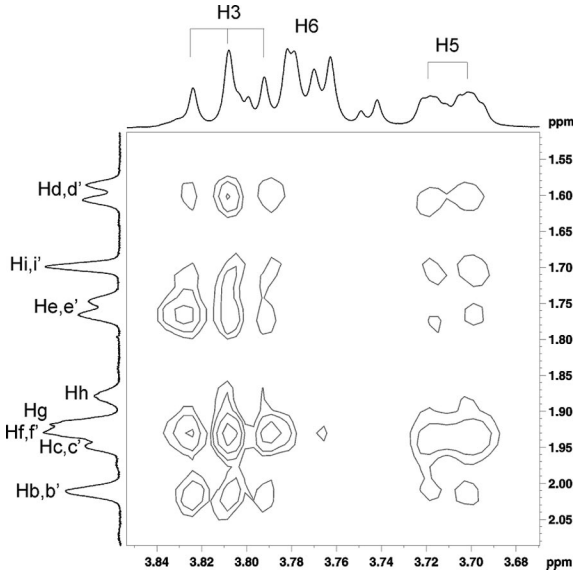


Figure 2. 600 MHz 2-D ROESY spectrum of **5**@β-CyD in $D_2O$. Mixing time 300 ms.

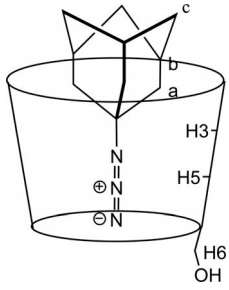


Figure 3. Proposed geometry of **1**@β-CyD in $D_2O$ based on 2-D ROESY measurements.

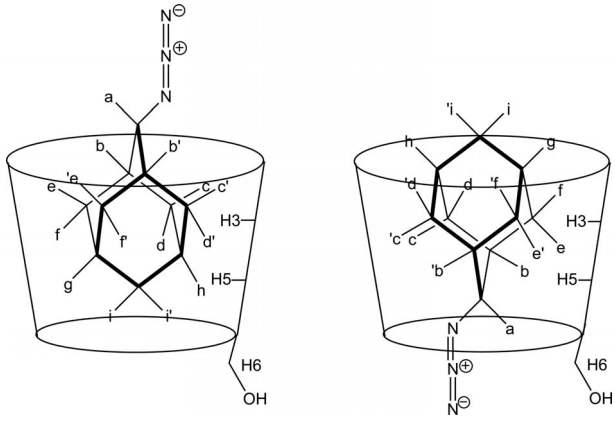


Figure 4. Proposed geometries of **5**@β-CyD in $D_2O$ based on 2-D ROESY measurements.

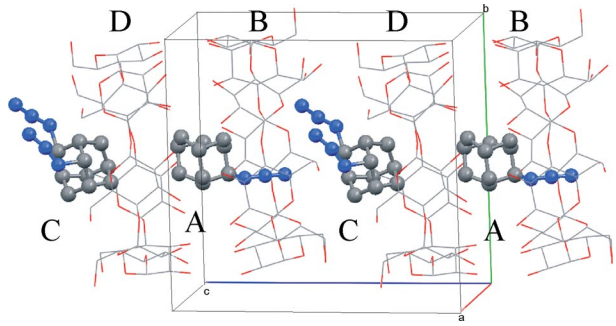


Figure 5. Single-crystal X-ray structure of **5**@β-CyD. Hydrogen and water molecules were removed for clarity. Two crystallographically independent β-CyD molecules B and D are present in the unit cell. The guest molecule C is disordered over two positions.[13]

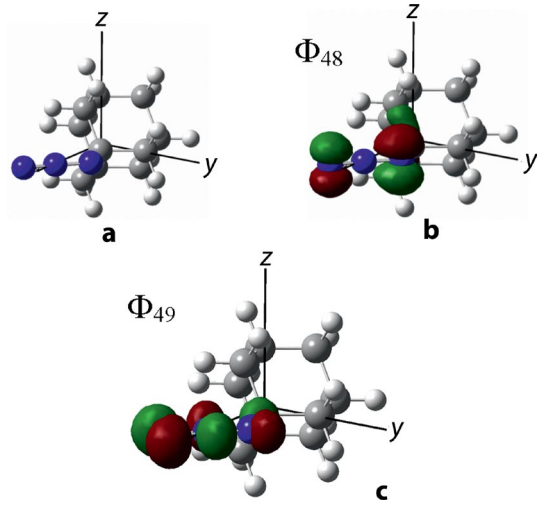


Figure 6. (a) B3LYP/6-31G(d)-optimized geometry of **1**, (b) HOMO, and (c) LUMO. Frontier orbitals involved in the TD/B3LYP/6-31G(d)-calculated transition at 283 nm based on B3LYP/6-31G(d)-optimized geometry (isosurface value 0.07).

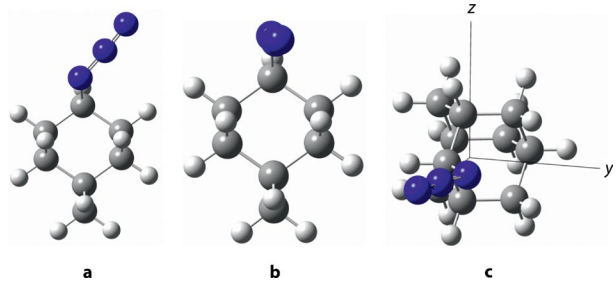


Figure 7. B3LYP/6-31G(d)-optimized geometries of **5**: (a) and (b) ground state geometric conformers, and (c) $C_s$ symmetric transition state between the two enantiomeric conformers of (a).

  

clinic non-centrosymmetric space group *P*1 (Figure 5). The unit cell consists of two crystallographically independent molecules of β-CyD (Figure 5, B and D). The first one accommodates a molecule of **5** with ca. 25% occupancy (Figure 5, A), and the second, a molecule of **5**, which is disordered over two positions with site occupation factors 0.5:0.5, with ca. 50% occupancy (Figure 5, C). The CyD molecules form channels with the dimers arranged in a head-to-head type fashion (Figure 5, for details see ref.[13]). Guest molecule A is entrapped between the wider apertures of CyDs D and B, which are mutually oriented in a head-to-head fashion. The azido group of A penetrates deeply into the cavity of B. On the other hand, the disordered guest C is not really confined, but only intercalated between B and D, which, in this case, are tail-to-tail oriented, e.g., the adamantane framework of C is located at the narrower aperture of CyD D.

Computations were performed to complement the X-ray structure (Figure 5). The gas-phase geometries of **1** (Figure 6) and **5** (Figure 7) were optimized with density functional theory (DFT), using Becke's[14] three-parameter hybrid method and the exchange functional of Lee, Yang, and Parr (B3LYP)[15] for a 6-31G(d) basic set. According to DFT, azide **5** can settle into two geometric minima (Figure 7, a, b) with **5a** being 3 kcal mol$^{-1}$ more stable than **5b**. In crystalline **5**@β-CyD, the guest adopts the more stable conformation of **5a** only.

Single-point calculations provided the UV/Vis electronic transition dipole moment vectors necessary for ICD spectra interpretation (vide infra). These single-electron vertical transitions of **1** and **5** were computed by two methods, i.e., single-excitation configuration interaction (CIS)[16] and time-dependent DFT (TD)[17] (Tables 2 and 3). The single-point calculations of **5** (Table 3) were performed based on its $C_s$-symmetric geometry (Figure 7, c), because this is the time-averaged geometry experienced in solution. This means that the molecule is rendered achiral due to the flipping of the azido group between the two enantiomeric conformers depicted in Figure 7 (a).

For the two azidoadamantanes investigated, only one electronic transition above $\lambda$ = 220 nm was found by TD and CIS methods with maxima at $\lambda \approx$ 280 nm, independent of the extent of configuration interaction (other transitions are not shown, Tables 2 and 3). As illustrated in the case of **1** (Figure 6, b, c), the frontier orbitals involved in the 283-nm transition (Table 2, TD method) are $\pi_z$–$\pi_y$* in nature. The TD calculation corroborates the former finding of a "perpendicular" $\pi_y$–$\pi_x$* transition in alkyl azides and azoimide.[18] As inferred from the transition dipole moment components shown in Tables 2 and 3, the transitions around 280 nm are *z*-polarized (perpendicularly to the C–N–N plane, where the azido group is positioned) for the investigated geometries of **1** and **5**. Both methods, CIS and TD, afforded similar results in terms of transition dipole moment vectors and energies of the $\pi_z$–$\pi_y$* transition.

The strengths of azidoadamantane (**1** and **5**):(α- and β-) CyD ICs were investigated using ICD in aqueous:ethanolic solutions at 293 K. Complexation of both **1** and **5** by β-CyD[19] produced negative signs of the ICD Cotton effect with a minimum at 285 nm (Figures 8 and 9). It should be noted that, due to the bimodal inclusion mode of **5**@β-CyD, interpretation of the negative ICD bands of **5**@β-CyD is complicated (vide infra).[20] The observed concentration dependencies were used to elucidate the types of ICs formed. The linear Scatchard plots[21] for both azidoadamantane@β-CyD ICs support 1:1 stoichiometries (Figures 10 and 11). Evaluation of the data also led to the determination of association constant ($K_a$) values.[22,23] The

Table 2. CIS(FC)/6-31G(d) and TD/B3LYP/6-31G(d) vertical transitions for **1** at the B3LYP/>6-31G(d) ground-state optimized geometry (Figure 6). Only the highest wavelength transition is shown.

| Method | Transition energy $\lambda$ [nm] | Orbitals involved | Orbital coefficient | Oscillatory strength *f* | Transition dipole moment components *x* | *y* | *z* |
|---|---|---|---|---|---|---|---|
| CIS | 281 | 28 → 49 | –0.10531 | 0.0001 | –0.0002 | 0.0004 | –0.0249 |
| | | 40 → 49 | 0.10877 | | | | |
| | | 46 → 49 | –0.13772 | | | | |
| | | 48 → 49 | 0.64961 | | | | |
| | | 48 → 51 | 0.11208 | | | | |
| TD | 283 | 48 → 49 | 0.68405 | 0.0000 | –0.0005 | 0.0001 | –0.0205 |

Table 3. CIS(FC)/6-31G(d) and TD/B3LYP/6-31G(d) vertical transitions for **5** at the B3LYP/6-31G(d) transition-state optimized geometry (Figure 7, C). Only the highest wavelength transition is shown.

| Method | Transition energy $\lambda$ [nm] | Orbitals involved | Orbital coefficient | Oscillatory strength *f* | Transition dipole moment components *x* | *y* | *z* |
|---|---|---|---|---|---|---|---|
| CIS | 280 | 27 → 49 | –0.10677 | 0.0001 | 0.0000 | 0.0000 | –0.0229 |
| | | 40 → 49 | 0.13669 | | | | |
| | | 45 → 49 | –0.15303 | | | | |
| | | 48 → 49 | 0.63976 | | | | |
| | | 48 → 51 | 0.12317 | | | | |
| TD | 283 | 48 → 49 | 0.68331 | 0.0000 | 0.0000 | 0.0000 | –0.0194 |

  

higher value of $K_a$(**1**@β-CyD) = 20240 ± 1000 $M^{-1}$ reveals that **1** is accommodated more tightly within the host cavity than is **5**, cf., $K_a$(**5**@β-CyD) = 7450 ± 400 $M^{-1}$.

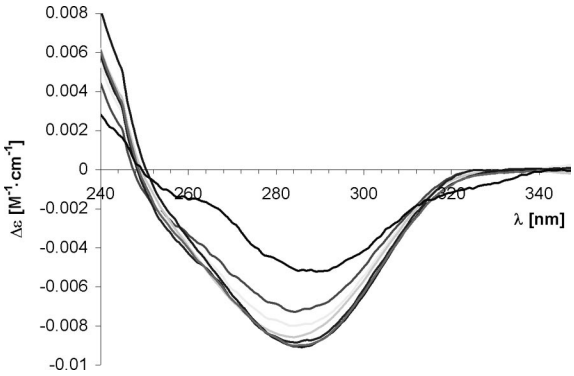


Figure 8. Concentration dependency for ICDs of **1**@β-CyD in $H_2O$/EtOH = 80:20 (v/v) at 293 K.

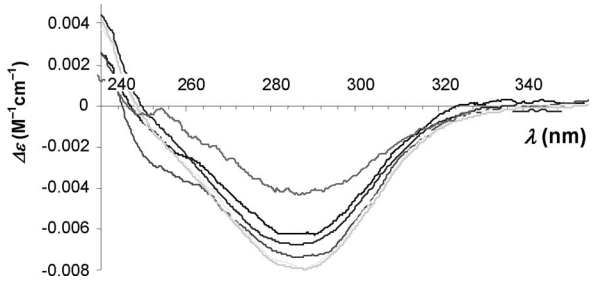


Figure 9. Concentration dependency for ICDs of **5**@β-CyD in $H_2O$/EtOH = 80:20 (v/v) at 293 K.

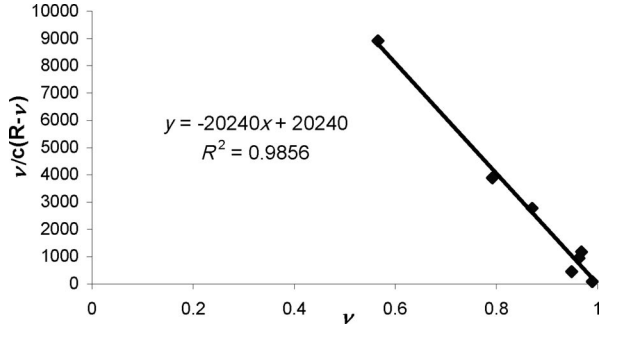


Figure 10. Scatchard plot for the determination of $K_a$ of the **1**@β-CyD IC in $H_2O$/EtOH = 80:20 (v/v) at 293 K. $K_a$(**1**@β-CyD) = 20240 ± 1000 $M^{-1}$.

The ICD spectrum for the IC of **1** and α-CyD produced two bands – a positive band with a maximum at 283 nm and a negative one with a minimum at 317 nm (Figure 12). Yet, that of **5** and α-CyD exhibited only one negative band with a minimum at 285 nm (Figure 13). Treatment of the ICD data of Figure 12 and Figure 13 by Scatchard plots led to a nonlinear phenotype (not shown), indicating an uneven stoichiometry. Indeed, the empirical compositions of the

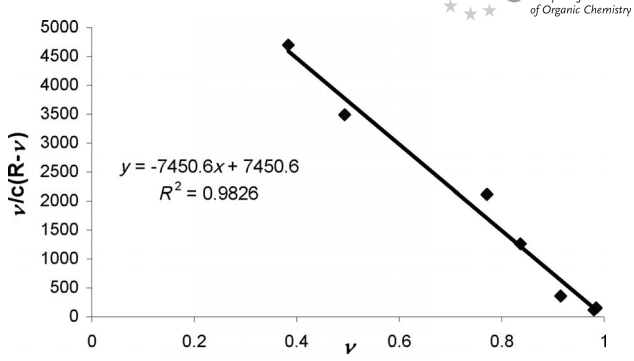


Figure 11. Scatchard plot for determination of $K_a$ of **5**@β-CyD in $H_2O$/EtOH = 80:20 (v/v) at 293 K. $K_a$(**5**@β-CyD) = 7450 ± 400 $M^{-1}$.

ICs of both **1** and **5** with α-CyD ICs were determined by NMR and microanalysis, which confirm 1:2 stoichiometries (see Table S1 of Supporting Information). A determination of $K_a$ values in these cases is very difficult and can generally only be conducted by making certain restricting assumptions.[22a,23]

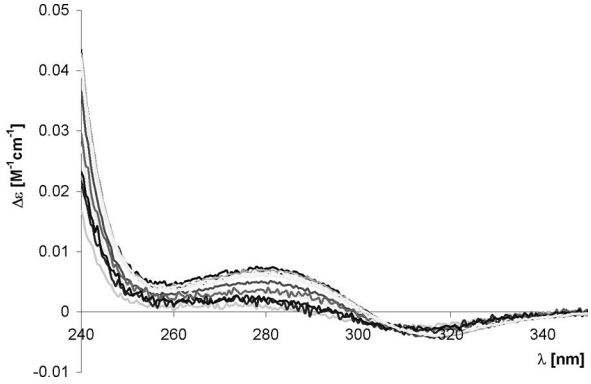


Figure 12. Concentration dependency for ICDs of **1**@(α-CyD)$_2$ in $H_2O$/EtOH = 90:10 (v/v) at 293 K.

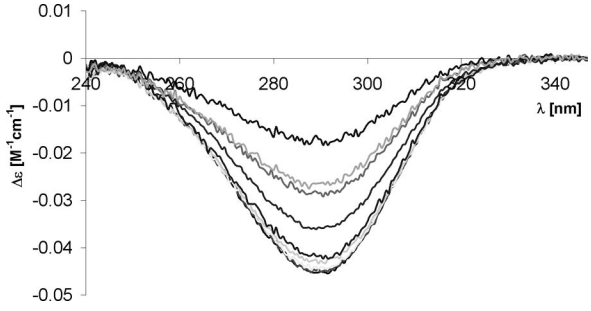


Figure 13. Concentration dependency for ICDs of **5**@(α-CyD)$_2$ in $H_2O$/EtOH = 90:10 (v/v) at 293 K.

According to 2-D ROESY measurements the adamantane framework in **1**@β-CyD is located above the host cavity while the azido group deeply penetrates into the β-CyD cavity. Harata's rule predicts a negative ICD when the transition dipole moment of the guest chromophore is

  

aligned perpendicular to the principal axis of the CyD cavity.[24] The development of this rule was based on aromatic π–π* transitions and later was validated for the d-d transitions of ferrocenes[25] and n–π* transition of the diazirine chromophore,[23] azoalkanes,[26] conjugated alkyl ketones,[27] and π–π* transitions of the azo group in azo dyes.[28] Here, the rule is being applied to the azide $\pi_z$–$\pi_y$* transition.[17] Thus, based on the geometry depicted in Figure 3, the azido chromophore should produce a negative ICD band, since the transition dipole moment vector of its 285-nm band is perpendicularly oriented to the C–N–N bond of the azido group (Table 2). Since negative ICD bands with a minimum at 285 nm were actually observed (Figure 8), the geometry proposed based on the 2-D ROESY technique correlates well with the ICD spectra.

## Conclusions

The product distributions from the photolyses of azidoadamantanes **1** and **5** included within CyD cavities were investigated in order to gain insight into the influence of supramolecular encapsulation. Upon photolysis of **1**@β-CyD as well as **1**@(α-CyD)$_2$, only amino alcohol **3** was formed. The lack of dimer **4** may be ascribed to classical solution chemistry, which entails hydrolysis of the intermediary bridgehead imine **2** embedded within the CyD cavity. Since azide **5** does not lead to a reactive imine, its incarceration did not alter its usual chemistry.

Investigation of the **5**@β-CyD supramolecular structure by 2-D ROESY NMR and single-crystal X-ray analysis revealed that **5** experiences a bimodal disposition within the cavity of β-CyD. ICD was used to determine the $K_a$ values of the ICs and to correlate their dispositions with 2-D ROESY NMR studies. In $H_2O$/EtOH = 8:2, 1-azidoadamantane (**1**) is bound more strongly to β-CyD than is 2-azidoadamantane (**5**). Azide **1** is nearly three times more strongly bound than azide **5** and is accommodated more tightly within the cavity. This correlates also with the nonhomogeneous orientations of **5** within β-CyD. The orientation of the transition dipole moment vector of the $\pi_z$–$\pi_y$* transition of the azido group was derived from DFT calculations. Subsequently, Harata's rule was applied to the geometry of **1**@β-CyD proposed by the 2-D ROESY technique and a close match was found between the experimental and predicted ICD signs. A generalization of this symmetry rule applicability on the transitions of the azido group would, however, require further elaborative and extensive analyses.

## Experimental Section

**General Procedure for the Preparation of Cyclodextrin Complexes:** A saturated cyclodextrin solution (5 equiv.) was placed into a high-walled beaker and azidoadamantane in ether was added in small amounts. The contents of the beaker were magnetically stirred and argon was simultaneously bubbled into the suspension through a needle for 8 h. Furthermore, the mixture was sonicated to disperse the organic azide and to protect against formation of clumps. The beaker was wrapped in aluminium foil to protect the starting material from light. The white suspension was filtered using a sintered funnel (porosity #4). The complex was dried at room temperature in a desiccator over $CaCl_2$ for 1 d at $P$ = 0.5 Torr. The approximate stoichiometry was inferred from integrals of $^1$H NMR spectra of complexes recorded in [D$_6$]DMSO.[29] The exact stoichiometries were determined by microanalysis based on nitrogen content and are summarized in Table 1 (see Supporting Information).

**Photolyses of Solid Cyclodextrin Complexes:** 100–300 mg of the solid complexes was weighed into a 250-mL round-bottom flask and dispersed over the entire inner surface. Using a manifold, the flask was evacuated and argon was allowed to replace the air (3×). The flask was closed quickly with a septum pierced with two cannulas (one being the inlet for argon and the other one the outlet). After a short flow of argon, the needles were removed and the septa wrapped with parafilm, then aluminum foil, and parafilm again to protect the septa against destruction by UV light. The rotating flask was immersed into an ultrasonic bath with circulating water (16–24 °C). The photolyses of the complexes were conducted by placing a medium-pressure mercury lamp (TQ718-Z4, 700 W, doped with $FeI_2$, glass jacket) beside the flask at a distance of 10–20 cm. The photolyses took 1–2 d depending on the amount of complex used. Occasionally, during the photolysis, a short sonication was applied to redistribute the solid complex over the walls of the flask, thereby exposing a fresh surface of complex towards the UV light. The low-molecular weight adamantane derivatives within the cyclodextrins were recovered by dissolving the product residue in water (100 mL) and dichloromethane (50 mL) and subjecting the mixture to continuous extraction with an apparatus for extracting liquids of higher density. After 24 h, the dichloromethane was replaced by a new portion to afford the first fraction and after 48 h a second dichloromethane extract was collected. In this way, the evaporation of potentially volatile products could be ascertained. The dichloromethane solutions were analyzed by GC–MS and the yields of the components were quantified by a GC-FID calibrated with (+)-camphor as an internal standard. Table 2 (see Supporting Information) summarizes the GC-FID data. After continuous extraction, water from the aqueous phase was evaporated in vacuo and analyzed for the presence of possible insertion or modification products formed by the reaction of CyD with adamantyl nitrene. All of the obtained CyD fractions, exhibited identical ESI-MS spectra and proved to be pure α- (see Figure S1 in the Supporting Information) or β-CyD (Figure S2).

The CyD fraction from the photolysis of azidoadamantane@α-CyD complexes were analyzed by RP-HPLC and LC-MS. No signals corresponding to the sum of adamantyl nitrene and α-CyD masses or related masses were found using the latter analysis. According to the RP-HPLC-RI analysis, the CyD fractions from the photolysis of the azidoadamantane:β-CyD complexes were found to be unaltered β-CyD.

**Determination of Association Constants by ICD Titration:** UV/Vis and CD spectra were recorded with a Lambda 16 spectrometer and a CD6 circular dichrograph, respectively, in thermostatted quartz cuvettes (10 cm path length). The ICD titration was done in $H_2O$/EtOH, 80:20 at 293 K by the dilution technique and subsequently, an iterative Scatchard plot for the $K_a$ determinations of 1:1 stoichiometric complexes of azidoadamantanes with β-CyD was used.[22,23] LINEST function was used for the assessment of the standard deviation of the linear Scatchard plot.

**Supporting Information** (see footnote on the first page of this article): ESI mass spectra, ICD titration data, and computations.

  

## Acknowledgments

This work was financially supported by the Fonds zur Förderung der wissenschaftlichen Forschung in Österreich (project number P12533-CHE). We thank Mr. A. Roller, Institut für Anorganische Chemie, Universität Wien, for performing X-ray measurements.

[1] a) *Organic Azides*: *Syntheses and Applications* (Eds.: S. Bräse, K. Banert), John Wiley & Sons, New York, **2010**; b) S. Bräse, C. Gil, K. Knepper, V. Zimmermann, *Angew. Chem. Int. Ed.* **2005**, *44*, 5188; c) A. Hassner, in: *Azides and Nitrenes: Reactivity and Utility* (Ed.: E. F. V. Scriven), Academic, New York, **1984**, pp. 35–76.

[2] a) M. S. Platz, in: *Reactive Intermediate Chemistry* (Eds.: R. A. Moss, M. S. Platz, M. Jones Jr), John Wiley & Sons, Hoboken, NJ, **2004**, pp. 501–559; b) E. F. V. Scriven, *Azides and Nitrenes*: *Reactivity and Utility*, Academic, New York, **1984**; c) C. Wentrup, *Reactive Intermediates*, John Wiley & Sons, New York, **1984**; d) W. Lwowski, *Nitrenes*, John Wiley & Sons, New York, **1970**.

[3] a) W. Lwowski, *Ann. N. Y. Acad. Sci.* **1980**, *346*, 491; b) E. L. Vodovozova, *Biochem. (Moscow)* **2007**, *72*, 1.

[4] G. Wagner, V. B. Arion, L. Brecker, C. Krantz, J.-L. Mieusset, U. H. Brinker, *Org. Lett.* **2009**, *11*, 3056.

[5] K. A. Connors, *Chem. Rev.* **1997**, *97*, 1325.

[6] J. Szejtli, *Chem. Rev.* **1998**, *98*, 1743.

[7] a) U. H. Brinker, R. Buchkremer, M. Kolodziejczyk, R. Kupfer, M. Rosenberg, M. D. Poliks, M. Orlando, M. L. Gross, *Angew. Chem. Int. Ed. Engl.* **1993**, *32*, 1344; b) For reviews, see: Mieusset, J.-L.; Brinker, U. H. *Encapsulation of Reactive Intermediates*. in: Molecular Encapsulation: Organic Reactions in Constrained Systems, U. H Brinker, J.-L. Mieusset, (Eds.), Wiley: Chichester, **2010**, pp. 269–308; c) M. G. Rosenberg, U. H. Brinker, *Eur. J. Org. Chem.* **2006**, 5423–5440; d) M. G. Rosenberg, U. H Brinker, *Carbenes Generated within Cyclodextrins and Zeolites*. in: *Adv. Phys. Org. Chem.* J. P. Richard (Eds.), Academic: New York **2005**, vol. 40, pp. 1–47.

[8] Complete hydrolysis to 7-(aminomethyl)bicyclo[3.3.1]nonan-3-one was not observed.

[9] a) H. Quast, P. Eckert, *Justus Liebigs Ann. Chem.* **1974**, 1727; b) I. R. Dunkin, C. J. Shields, H. Quast, B. Seiferling, *Tetrahedron Lett.* **1983**, *24*, 3887; c) J. Michl, G. J. Radziszewski, J. W. Downing, K. B. Wiberg, F. H. Walker, R. D. Miller, P. Kovacic, M. Jawdosiuk, V. Bonacic-Koutecky, *Pure Appl. Chem.* **1983**, *55*, 315.

[10] a) D. Krois, L. Brecker, A. Werner, U. H. Brinker, *Adv. Synth. Catal.* **2004**, *346*, 1367; b) W. Knoll, M. M. Bobek, G. Giester, U. H. Brinker, *Tetrahedron Lett.* **2001**, *42*, 9161.

[11] T. Sasaki, S. Eguchi, N. Toi, *J. Org. Chem.* **1979**, *44*, 3711.

[12] D. Krois, M. M. Bobek, A. Werner, H. Kählig, U. H. Brinker, *Org. Lett.* **2000**, *2*, 315.

[13] CCDC-802794 contains the supplementary crystallographic data for this paper. These data can be obtained free of charge from The Cambridge Crystallographic Data Centre via www.ccdc.cam.ac.uk/data_request/cif.

[14] A. D. Becke, *J. Chem. Phys.* **1993**, *98*, 5648.

[15] C. Lee, W. Yang, R. G. Parr, *Phys. Rev. B* **1988**, *37*, 785.

[16] J. B. Foresman, M. Head-Gordon, J. A. Pople, M. J. Frisch, *J. Phys. Chem.* **1992**, *96*, 135.

[17] M. E. Casida, C. Jamorski, K. C. Casida, D. R. Salahub, *J. Chem. Phys.* **1998**, *108*, 4439.

[18] W. D. Closson, H. B. Gray, *J. Am. Chem. Soc.* **1963**, *85*, 290. The arbitrary designation of π orbitals in terms of reference axes as *x*, *y*, *z* in our system are *y*, *z*, *x*, respectively.

[19] *Handbook of Cyclodextrins and Their Complexes* (Ed.: H. Dodziuk), Wiley-VCH, Weinheim, Germany, **2006**.

[20] For calculations of ICD spectra and subsequent correlations with ICD, see: a) G. Marconi, B. Mayer, *Pure Appl. Chem.* **1997**, *69*, 779; b) B. Mayer, X. Zhang, W. M. Nau, G. Marconi, *J. Am. Chem. Soc.* **2001**, *123*, 5240.

[21] C. R. Cantor, P. R. Schimmel, *Behavior of Biological Macromolecules* (Ed.: W. H. Freeman), San Francisco, **1980**, part III, p. 849.

[22] a) D. Krois, U. H. Brinker, *J. Am. Chem. Soc.* **1998**, *120*, 11627; b) D. Krois, U. H. Brinker, *Circular Dichroism of Cyclodextrin Complexes*, in: *Handbook of Cyclodextrins and Their Complexes* (Ed.: H. Dodziuk ), Wiley-VCH, Weinheim, Germany, **2006**, pp. 289–298.

[23] M. M. Bobek, D. Krois, U. H. Brinker, *Org. Lett.* **2000**, *2*, 1999.

[24] K. Harata, H. Uedaira, *Bull. Chem. Soc. Jpn.* **1975**, *48*, 375.

[25] a) A. Harada, S. Takahashi, *Chem. Lett.* **1984**, 2089; b) A. Harada, Y. Hu, S. Yamamoto, S. Takahashi, *J. Chem. Soc., Dalton Trans.* **1988**, 729; c) V. I. Sokolov, V. L. Bondareva, I. F. Golovaneva, *J. Organomet. Chem.* **1988**, *358*, 401; d) V. I. Sokolov, V. L. Bondareva, I. F. Golovaneva, *Metalloorganicheskaya Khimiya* **1988**, *1*, 716) (for the Engl. translation, see: *Organomet. Chem. USSR* **1988**, *1*, 400e) N. Kobayashi, M. Opallo, *J. Chem. Soc., Chem. Commun.* **1990**, 477.

[26] H. Bakirci, X. Zhang, W. M. Nau, *J. Org. Chem.* **2005**, *70*, 39, and references cited therein.

[27] G. M. Bonora, R. Fornasier, P. Scrimin, U. Tonellato, *Carbohydr. Res.* **1986**, *147*, 205.

[28] a) M. Suzuki, M. Kajtar, J. Szejtli, M. Vikmon, E. Fenyvesi, L. Szente, *Carbohydr. Res.* **1991**, *214*, 25; b) Y. Liu, Y.-L. Zhao, H.-Y. Zhang, Z. Fan, G.-D. Wen, F. Ding, *J. Phys. Chem. B* **2004**, *108*, 8836.

[29] The inclusion complex is fully dissociated in dilute DMSO solutions and the $^1$H NMR spectrum may be interpreted as a sum of proton spectra of the neat components.

Received: November 12, 2010
Published Online: January 12, 2011

  